Available online at www.sciencedirect.com
SCIENCE DIRECT®
Carbohydrate Polymers 57 (2004) 153–163
Carbohydrate Polymers
www.elsevier.com/locate/carbpol

Rheological characterisation of the gelation behaviour of maltodextrin aqueous solutions

Chrystel Loret[a,*], Vincent Meunier[a], William J. Frith[a], Peter J. Fryer[b]

[a]*Unilever R&D Colworth, Colworth House, Sharnbrook, Bedford MK40 1DG, UK*
[b]*Centre for Formulation Engineering, Chemical Engineering, University of Birmingham, Edgbaston, Birmingham B15 2TT, UK*

Received 9 September 2003; revised 5 February 2004; accepted 25 March 2004

Available online 20 July 2004

Abstract

As a prelude to the study of its co-gelation with other biopolymers, the gelation behaviour of maltodextrin Paselli SA2 has been investigated in detail. Our work extends that done previously and leads to a number of interesting new findings, regarding maltodextrin gel behaviour. Studies were made of the effect of maltodextrin concentration and temperature on gelation using viscosity, small amplitude oscillatory and spectrophotometry measurements. Our results show that the c^* concentration is close to the critical gelation concentration and in the region of 17%. A linear equation relating the three parameters, gel time, concentration and gelation temperature is obtained. Data obtained from rheology experiments also allow master curves to be constructed, which can be used to predict gel behaviour for any concentration or gelation temperature in the range studied. We find that the cascade model cannot be applied to our results for maltodextrin gelation. This is probably due to gelation being more closely related to a colloidal aggregation. Furthermore, a study on the influence of temperature of dissolution points out an optimum dissolution temperature leading to a quicker and stronger gel. The effect is not well understood but the presence of nuclei (aggregates of double helices of amylose) is a possible explanation.

Keywords: Maltodextrin; Gelation; Master curve

1. Introduction

The increasing trend in nutritional and health awareness has lead to a strong demand from the consumer for reduced or low-fat foods. However, fat contributes significantly to the sensorial properties of food products in a variety of ways. Hence, the physico-chemical properties of fats are key aspects of food texture, which substitutes should mimic, if they are to be effective. Maltodextrins are one of the most popular types of fat replacers that have been introduced as food additives in the last 25 years.

Maltodextrins are a hydrolysis product of starches that have dextrose equivalent (DE) values lower than 20. Here, the DE is defined as the total number of reducing sugars relative to a glucose baseline of 100 and is expressed on a dry-weight basis. Hydrolysis products with a DE above 20 are generally referred to as 'glucose syrups', which, as the name implies are liquids supplied in the form of aqueous solutions. It is, in part, the solubility of the hydrolysis product that distinguishes the two classes of material, i.e. above a DE of 20, the product is made of short oligomers that are freely soluble in water, whereas below 20 there is a sufficient proportion of long polymeric chains to inhibit solubility and promote gelation (Ritcher, Schierbaum, Augustat, & Knoch, 1976). It is clear, then, that maltodextrins are complex mixtures of high and low molecular weight materials. The nature of the starch hydrolysis, and the process used will have an important influence on the composition and properties of final product and its gel. Processes used include acid hydrolysis (Robin, Mercier, Charbonniere, & Guilbot, 1974), enzymatic hydrolysis, or a combination of both methods. The maltodextrin under investigation here is a polysaccharide produced by α-amylase enzymatic degradation at the gelatinisation temperature of native potato starch. Maltodextrins produced in this way contain a proportion of linear amylose in a broad range of molecular weights. However, the majority of the material is amylopectin that has a branched structure.

* Corresponding author. Tel.: +44-1234-222-983; fax: +44-1234-222-757.
E-mail address: chrystel.loret@unilever.com (C. Loret).

0144-8617/$ - see front matter © 2004 Elsevier Ltd. All rights reserved.
doi:10.1016/j.carbpol.2004.03.026

The capacity of maltodextrin to reproduce the fat-like mouthfeel presumably originates from the three-dimensional network that maltodextrins show when gelled and understanding the nature of this network has been the focus of a number of studies. Using low-resolution H-NMR, Schierbaum et al. (1992) have shown that the linear amylose fraction in the dissolved state is responsible for the initiation and acceleration of maltodextrin gel formation. The outer linear chains of amylopectin are thought to interact with amylose, thus reducing their self-association, and leading to the formation of a hydrated common network. This hypothesis of a 'synergistic' interaction mechanism between the different fractions is also confirmed by Bulpin, Cutler, and Dea (1984). Reuther et al. (1984) has expanded on this, proposing the following gelation mechanism: at sufficiently high concentration of macromolecules, isolated double helices are formed from linear amylose, and sufficiently long linear segments of branched molecules. These double helices aggregate to form crystalline domains, which are suspended in a polymer solution with disordered chain segments. Some of the macromolecules are sufficiently long to connect different crystalline domains, thus forming the junction zones of the network.

These crystallites have been characterised using small and wide-angle X-ray scattering (Gernat, Reuther, Damaschun, & Schierbaum, 1987; Reuther et al., 1984). Reuther et al. (1983) have demonstrated the presence of regions of high and low density in the maltodextrin gels. These regions have the shape of flat discs with a maximum diameter of almost 280 nm, a height between 28 and 36 nm and an average radius of gyration of 90 nm. As shown by wide-angle X-ray scattering of the gel, the regions have a crystalline structure similar to that of the B-form of amylose. The polymer chains are arranged in double stranded helices, which are packed in a hexagonal unit cell (Reuther et al., 1984).

Kasapis, Morris, Norton, and Clark (1993) have already shown that the sol–gel transition is a slow process, which depends on the temperature and concentration. To do so, they employed a simple visual method to determine the time required for formation of a self-supporting network: the samples were inverted, and the time required to form a gel strong enough to withstand this was recorded. Only selected samples were monitored more rigorously by mechanical spectroscopy. In the present work, a more extensive study on the effect of concentration and temperature on maltodextrin gelation was conducted under small amplitude deformation. These results yield information on the mechanism of maltodextrin gelation. Also, viscosity measurements of maltodextrin solutions gave information on the dilute and concentrated regime transition. The influence of the temperature of dissolution was also for the first time investigated and showed that there is an optimum preparation condition for this biopolymer.

2. Material and methods

2.1. Material

The food grade maltodextrin used in these experiments was obtained from Avebe (The Netherlands). Paselli SA2 is an enzymatically converted potato starch-based product, with a DE less than 3 and a pH between 5.5 and 7 in aqueous solution. It is available as a white powder, with a moisture content less than 9%. 99.7% of the carbohydrates have a degree of polymerisation greater than 3. There is no glucose present in the sample.

The size distribution of the Paselli SA2 was characterised by high-performance size-exclusion chromatography (HPSEC) using Anagel-TSK PW_{XL} G4000, G5000 and G6000 columns in series, in combination with a TSK PW_{XL} guard column, maintained at 60 °C. The mobile phase was an aqueous solution of 0.1 M $NaNO_3$ and the flow rate was 0.5 ml/min. The size-exclusion pattern shows a bimodal distribution, with a low-molecular weight peak of $(1.029 \pm 0.008) \times 10^4$ g/mol and a high-molecular weight peak of $(4.92 \pm 0.02) \times 10^5$ g/mol. Both peaks show a high polydispersity index, respectively, 2.86 ± 0.01 and 2.25 ± 0.02.

2.2. Methods

2.2.1. Preparation of SA2 solution

The required quantity of solvent was weighed into a bottle and stirred at room temperature while the maltodextrin powder was poured in progressively. After 10 min, the solution was immersed and stirred in a water bath at different temperatures (80–120 °C) during 30 or 90 min. For solutions prepared at higher temperature than 100 °C, a pressure cooker was used. All the concentrations were prepared weight per weight (w/w). The main solvent used was distilled water (18.2 MΩ/cm). The maximum concentration investigated was 40%, difficulties were experienced in preparing uniform solutions at higher concentrations than this.

2.2.2. Rheological measurements

2.2.2.1. Viscosity measurement. Viscosity curves were obtained using the Low Shear 30 rheometer (Contraves), a concentric cylinder viscometer. Measurements were made in the shear rate range $0.1–100\ s^{-1}$. To avoid gelation, the studies were carried out at 60 °C. One minute was allowed between measurements for the reading to reach a constant value.

The measured viscosities were used to analyse the concentration-dependent behaviour of the solution. Plotting the specific viscosity versus the concentration on a log–log scale allows us to distinguish the semi-dilute regime from the dilute regime. The specific viscosity, η_{sp} is the fractional increase in viscosity due to the presence of the solute and is

defined as

$$\eta_{sp} = (\eta - \eta_{sv})/\eta_{sv} \quad (1)$$

where η_{sv} is the viscosity of the solvent.

2.2.3. Small amplitude oscillatory measurements

Oscillatory measurements were obtained using an ARES controlled strain rheometer (Rheometrics) equipped with a concentric cylinder-measuring cell. The dimensions of the cylinder used were $R_{cup} = 17$ mm, $R_{bob} = 16$ mm and $h_{bob} = 33.3$ mm. Parallel plates (25 mm diameter) were used for solutions at high concentrations (35–40%), i.e. when the measured torque produced by the concentric cylinder geometry was too high.

It was decided to quench the sample, rather than using a temperature ramp, as this facilitates analysis of the gel time. Hot maltodextrin solution was poured immediately into the coaxial cylinder that was already at the desired gelation temperature, which varied from 5 to 40 °C. In this way, the fastest quench was achieved. Samples were covered with mineral oil to prevent evaporation during the measurements.

To determine the strain and frequency-dependent behaviour of the gels, strain sweeps were carried out from 0.1 to 1.8% at 1 rad/s frequency, and at concentrations up to 40%. These measurements showed that G' and G'' have constant values from 0.1 to 0.5% strain, over the entire concentration range studied. Therefore, frequency sweeps were performed from 10^{-2} to 10^{2} rad/s at 0.5% strain. The measurements were performed 5 h after the sample was poured into the Couette geometry. In addition, the evolution of G' and G'' was followed as a function of time. Time-dependent oscillatory measurements were made at 0.5% strain and 1 rad/s frequency: 0.5% strain was chosen since it is near the upper limit of linear behaviour for the gels, so as to give the best possible precision in measuring the gelation kinetics, but still remain within the linear regime for all concentrations.

Following previous studies (Doublier and Choplin, 1989; Kasapis et al., 1993; Vorwerg and Radosta, 1995), the gel time was defined as the point when the elastic response (G') became greater than viscous response (G''). Although Winter and Chambon (1986) have shown that using this criterion can result in a frequency-dependent gel time, the possible error for our system is small (of the order of the time between the measurement points). Hence, it was felt that using the same method as used by previous workers was preferable. In all cases, the time taken to load the sample and start the experiment was shorter than the shortest measured gel time. The moment the bob was loaded into the cup was taken as the start point.

For many biopolymers (amylose (Doublier and Choplin, 1989), carrageenan (Meunier, Nicolai, Durand, & Parker, 1999), gelatin (Normand, Muller, Ravey, & Parker, 2000a)) it has been shown that, in double logarithmic plotting, storage modulus as a function of time was increasing in two steps: (i) a fast stage, corresponding to associative mechanisms and network formation, followed by (ii) a much slower process, which may follow a power law with time, due to large scale reorganisations. In this power law regime, when the exponent is small enough, the evolution of $\log(G')$ versus 1/time can be considered linear, and a value can be approximated for infinite time. To do so, we have plotted the log of the storage modulus (taken in the long time linear regime) versus 1/time. An extrapolation toward zero gives G'_{inf}, the storage modulus at infinite time, as shown in Fig. 1. The main advantage of this method is to give a good estimate of G' for non-accessible experiment times. Nevertheless, we are making the assumption here that the storage modulus will reach an equilibrium state. Thus, since in the long-time regime, cure curves exhibit power law dependence with time, extrapolation to a finite value, G'_{inf}, should be treated with caution. In Fig. 1, it is worth noting that the slope of the evolution of $\log(G')$ with 1/time can be related to the kinetics of gelation. For low temperatures, the kinetics are fast, and the slope is close to zero. For higher temperatures, gelation becomes very slow, and the slope increases accordingly.

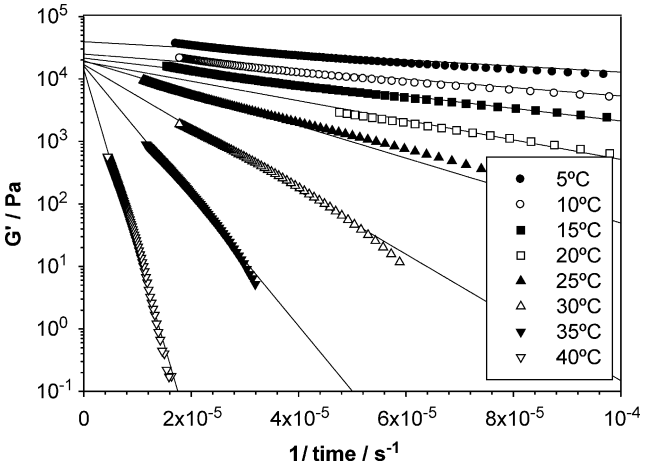

Fig. 1. Determination of G'_{inf} by plotting G' as a function of 1/time for 25% (w/w) SA2 sample quenched at different temperatures (Strain amplitude: 0.5%, Frequency amplitude: 1 rad/s).

2.2.4. Spectrophotometry

The optical density experiments were carried out using a UV/VIS lambda 40 (Perkin Elmer) spectrophotometer. Hot maltodextrin solution was poured into a quartz cell with an optical path of 0.5 cm, which was already set at the gelation temperature. The optical density, relative to that of pure water was recorded at 400 nm as a function of time.

3. Results and discussion

3.1. Characterisation of SA2 solutions by viscosity measurements

Fig. 2 shows the viscosity curves of SA2 at different concentrations (1–35%). At 60 °C, solutions exhibit

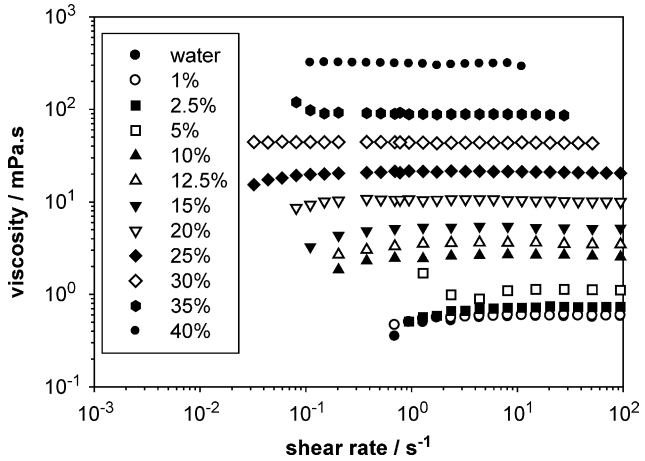

Fig. 2. Viscosity curves of SA2 samples at different concentrations (Contraves rheometer, 60 °C).

a Newtonian behaviour in the range of concentrations studied. The non-linear behaviour at low shear rates is mainly due to the limited sensitivity of the instrument.

From these data, specific viscosities can be calculated. The behaviour of the specific viscosity as a function of concentration is shown in Fig. 3. The concentrations in weight per weight (w/w) were converted to g/dl, assuming that all solution densities were equal to 1 g/ml.

Many literature studies (Launay, Doublier, & Cuvelier, 1986; Morris, 1984) have revealed that the concentration dependence of the specific viscosity shows two regions of power law behaviour on either side of the overlap concentration c^*. Power law values for the two regions for different linear biopolymers (guar gum, locust bean gum, alginate, etc.) have been reported in the range 1.1–1.4 in the dilute regime, and 3.5–5.1, in the concentrated regime. For maltodextrin, at low polymer concentration, the specific viscosity increases with a power law exponent of 1.4. At higher concentrations, a power law exponent of 4.7 is found, although the fit is not as good as at low concentrations. The point at 15% SA2 is not taken in account in the determination of the two regimes as it falls within the region of uncertainty around the c^* (17%).

It is interesting to note that such a complex and branched polymer as maltodextrin behaves like a linear polymer in terms of power laws. The value for c^*, however, is much bigger than is generally observed for other biopolymers. For example, the coil overlap concentration for κ-carrageenan (0.1 M NaCl, pH 9) is 0.45% (g/l) (Croguennoc, Meunier, Durand, & Nicolai, 2000), for guar gum 0.22% (g/l), for alginate (0.2 M NaCl) 1% (g/l) and for dextran 8% (g/l) (Morris, Cutler, Ross-Murphy, & Rees, 1981).

For most polymer chains, a shear-thinning behaviour is observed above c^*, due to the disentanglement and orientation of chains at higher stresses. However, in the case of SA2, solutions above c^* still exhibit a Newtonian behaviour. These observations could be explained by the branched structure of amylopectin and the polydispersity in the molecular weight of the sample. As described in Section 2, for both high and low molecular weight fractions, the polydispersity is larger than 2.

3.2. Gelation behaviour of SA2

A typical example of the variation of the storage modulus, G', and the loss modulus, G'', during the gelation process is shown in Fig. 4 for 25% SA2, quenched at 10 °C. Also shown are the results from the spectrophotometry study.

From Fig. 4, the process of SA2 gelation at 10 °C could be described as follows: during a first induction period, the medium remains clear and the rheological response fluid-like ($G' < G''$). Shortly after this (7 min), particles are formed and the optical density increases. Reuther et al. (1984) have shown by wide-angle X-ray measurements that the maltodextrin gel is composed of disk-like crystalline domains. Therefore, the turbidity increase could be interpreted as the nucleation of these crystallites since it occurs on a rather short time scale (within 7 min) and before

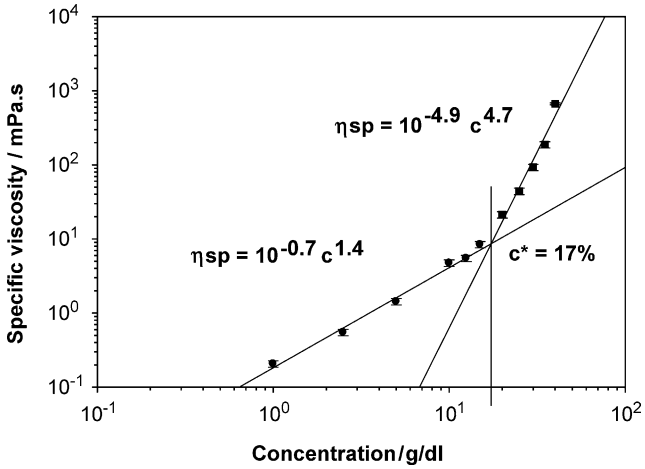

Fig. 3. Specific viscosity of SA2 samples versus concentration (Contraves rheometer, 60 °C).

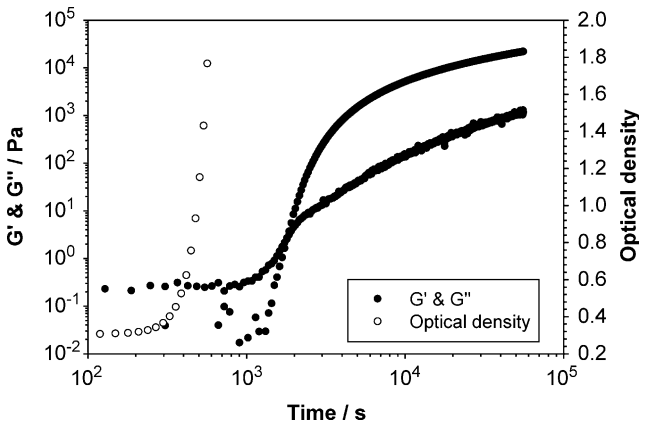

Fig. 4. Comparison of variation of G' and G'' (Strain amplitude: 0.5%, frequency amplitude: 1 rad/s, T_{gel}: 10 °C) and evolution of optical density ($\lambda = 400$ nm) as a function of time for 25% (w/w) SA2 sample.

gelation. During this period the rheology remains largely unchanged. It is not until 25 min after the temperature quench that a network is formed (as indicated by a rise in G'), implying that the crystallites formed are the building blocks from which the gel arises. The third period is characterised by a slowing of the rate of increase of G'. However, despite the long time over which data were acquired, it is clear that the kinetics of SA2 gel formation is slow and the gel does not reach a final state in the time scale investigated (13 h). This period is probably governed by a further crystallisation or rearrangement, but diffusion of macromolecules is slowed due to the high viscosity of the medium.

Fig. 5 shows the frequency dependence of G' and G'' of a 25% (w/w) SA2 gel, 5 h after the gel time. There is no variation in G' within the experimental range of frequency, that is between 10^{-2} and 10^{+2} rad/s and the value of G' is one or two orders of magnitude greater than that of G''. These results support the view that this system is an elastic 'true' gel (Morris, 1984). The value of G'' goes through a minimum at a frequency of around 0.2 rad/s. This minimum in G'' over the experimental frequency range has also been observed in a cross-linked starch gel (GluckHirsch & Kokini, 1997), κ-carrageenan (Meunier et al., 1999) and gelatin gels (Richardson, Robinson, Ross-Murphy, & Todd, 1981). Ferry (1980) has argued that the minimum in G'' can arise from the presence of two relaxation time-scales in the network: one, at high frequencies, or short time-scales, that arises from relaxation processes in between junction zones in the network, and the other that arises from relaxation processes of the network itself. Whilst Ferry was clearly referring to entangled or cross-linked polymer networks in his discussion, it seems likely that such a separation of timescales can also occur in biopolymer associative, and colloidal networks, although due to a somewhat different molecular process, and it is likely that it is such a separation of time-scales that is occurring in the current data. This aspect of the SA2 gel network behaviour has previously been discussed in more detail by Manoj, Kasapis, and Chronakis (1996) and Manoj, Kasapis, and Hember (1997).

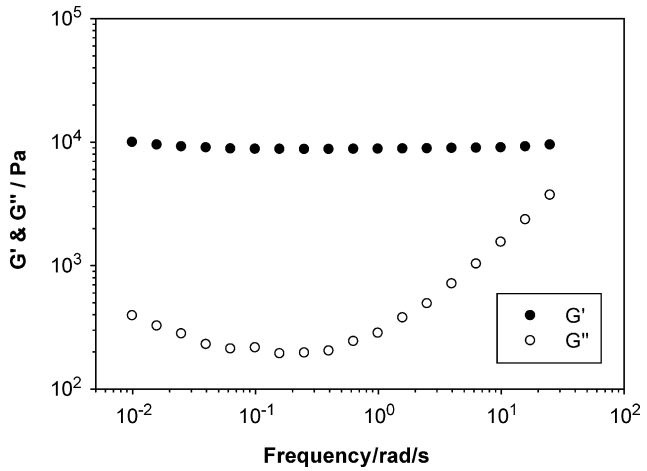

Fig. 5. G', G'' as function of frequency for 25% (w/w) SA2 sample after 5 h (strain amplitude: 0.5%, T_{gel}: 10 °C).

3.3. Effect of preparation temperature on 25% SA2

3.3.1. Influence of temperature of dissolution on 25% SA2

Usually, gel moduli and other rheological properties depend on the temperature profile during the formation of the gel. The dissolution temperature, however, is not considered to have a strong influence on the rheological properties if preparations are carried out at a temperature higher than the critical temperature of dissolution. However, this appears not to be the case for SA2, as our results demonstrate below.

25% SA2 solutions were prepared at different temperatures from 80 to 120 °C, and at two dissolution times (30 and 90 min). Their gelation was followed by mechanical spectrometry at 10 °C. The results are shown in Fig. 6 and it appears that there is an optimum in dissolution temperature leading to a quicker gelation ($t_{G'=G''}$ smaller) and stronger (G' at $t = \infty$ bigger) gel. The same trend was observed for both dissolution times, though there is a shift of the optimum towards lower temperatures if the solution is dissolved for longer, indicating a kinetic effect in the dissolution process.

It is not clear what causes this behaviour, but the presence of nuclei (aggregates of double helices of amylose) is a possible explanation. Gernat et al. (1987) have shown that the crystalline domains in the disk-like regions of the maltodextrin network do not consist of ideal crystals, but that lattice distortions exist inside the crystal structure that are composed of many microcrystallites. Ten to 16% of the carbohydrate chains may be involved in these crystallites, which are 16–17 nm in size, independent of concentration. It may be that these small domains are evidences of the presence of nuclei in the solution. The size and concentration of nuclei might then depend on the temperature of dissolution. Microscopic observations were not conclusive because the nuclei were too small to be observed.

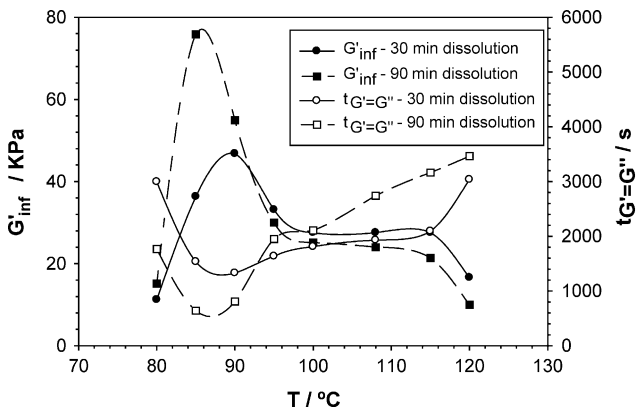

Fig. 6. Effect of temperature of dissolution during 30 or 90 min on G' value at $t = \infty$, G'_{inf}, and gel time of 25% (w/w) SA2 sample (strain amplitude, 0.5%; frequency amplitude: 1 rad/s, T_{gel}: 10 °C).

Another experiment, which supports this hypothesis, is the study of the re-melting of the gel. Previous studies (Manoj et al., 1997) have shown that melting and re-cooling of a previously formed maltodextrin gel leads to more rapid gelation kinetics, presumably due to the presence of nucleation sites formed during the first gelation sequence. Further investigations were made of the extent to which an SA2 gel recovers after re-melting, that employed a higher melting temperature than had previously been reported (Manoj et al., 1997). Recovery was studied by first measuring the cure curve of a 25% SA2 sample for 5 h at 10 °C. During this time, the remaining sample was kept in a fridge at 4 °C and then heated to 100 °C for 30 min, after which gelation was studied as described above. After melting the gel, the solution gels more quickly and gives a stronger gel. This result provides evidence that the gelation kinetics are heavily influenced by the presence of nuclei, and that after melting of a previously formed gel, there may be more nuclei present in the solution, which more quickly initiate gelation. In addition, the fact that the nuclei are apparently able to survive being heated to 100 °C adds weight to the argument that nuclei are responsible for the observed dependence of gel properties on dissolution temperature.

The mechanism of formation of the nuclei is unclear. It may be that they are present in the powder in an aggregated form, and these aggregates increasingly break up as the temperature increases. Alternatively, they may form from amorphous material, that orders as it is hydrated. Whatever the mechanism, it seems clear that up to 90 °C, increasing the temperature makes more nuclei available. This is based on the idea that more nuclei create a larger number of smaller crystallites, which in turn lead to a more rapidly forming, stronger gel. Increasing the temperature between 90 and 110 °C causes more of the nuclei to disappear. At higher temperatures (above 110 °C), the ordered helices could also transform to disordered coils. This presumably explains the shape of the curve above 110 °C. Moates, Noel, Parker, and Ring (1997) have shown that the dissolution temperature of the B-crystalline polymorph of amylose strongly depends on chain length, and at $T > 100$ °C, a chain length of 40 can be dissolved, although a temperature higher than 140 °C is necessary to dissolve aggregated amylose completely (Clark, Gidley, Richardson, & Ross-Murphy, 1989).

On the basis of the data in Fig. 6, 100 °C during 30 min was chosen as the experimental dissolution condition for the rest of the studies, since here the gel properties are less sensitive to temperature and time fluctuations.

3.4. Influence of temperature of gelation on 25% SA2

25% SA2 solutions were quenched to different temperatures in the rheometer, and the evolution of G' and G'' were followed over time. Results are shown in Fig. 7. Variations in G'' are not shown, as they show the same trend as Fig. 4.

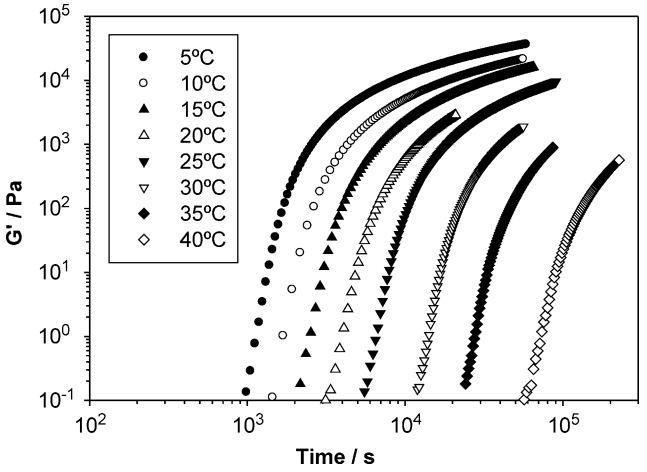

Fig. 7. Influence of temperature on gelation behaviour of 25% (w/w) SA2 sample (strain amplitude: 0.5%, frequency amplitude: 1 rad/s).

Gelation is much faster at low than at high temperatures, which is probably due to a change in the crystallisation rate. According to German, Blumenfeld, Guenin, Yuriev, and Tolsguvoz (1992) a decrease in temperature may decrease the thermodynamic quality of the solvent, which favours the formation of the structural elements of the gels, the crystallites. This observation is confirmed by plotting the gel time versus the temperature of gelation (Fig. 8). The gel time increases with the temperature of gelation, showing an apparent divergence in the region of 40 °C. Two kinetic phenomena seem to govern the behaviour: the kinetics of crystallisation and that of gelation. At high temperatures, the mechanism involved is slower and may be governed by the kinetics of the crystallisation. At low temperature, the kinetics of gelation may overcome the kinetics of crystallisation and gelation may occur before crystallisation can finish. This hypothesis is supported by the following observation. A sample of 25% was left at 50 °C in an oven for 2 weeks. The solution becomes opaque white but when the flask was turned upside down the sample flowed,

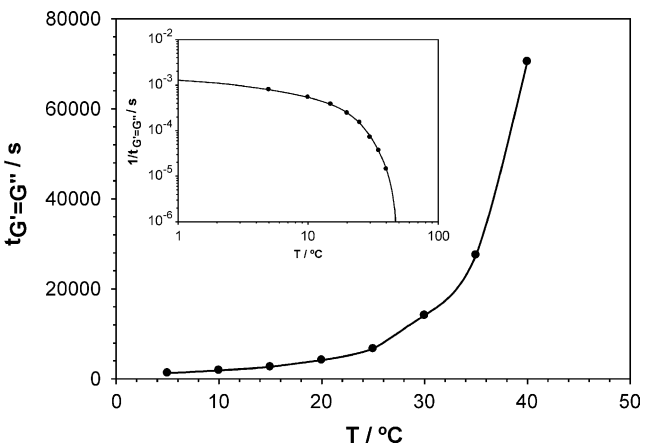

Fig. 8. Temperature-dependence of gel time of 25% (w/w) SA2 sample (amplitude strain: 0.5%, amplitude frequency: 1 rad/s). The insert presents the gelation temperature-dependence of $1/t_{G'=G''}$ of 25% (w/w) SA2 sample.

indicating that crystallisation occurs but gelation does not. It appears that crystallisation and gelation are two different processes and crystallisation does not necessary result in gelation. It seems, therefore, that the critical temperature of gelation must be lower than the temperature of crystal formation. By plotting $1/(t_{G'=G''})$ against the temperature, we can estimate the critical gelation temperature of SA2 (insert Fig. 8), which is around 50 °C, which supports the previous observations. An arbitrary function was used for this extrapolation, when $1/(t_{G'=G''})$ is plotted versus $(1/T)$ with T in Kelvin, to check if maltodextrin gelation follows the Arrhenius law, a linear relation was not found. A double Arrhenius relation was also tested but did not fit the experimental behaviour.

The influence of gelation temperature on G'_{inf} is much weaker than on gel time, indicating that the final gel state is relatively unaffected by the temperature of gelation, below the critical gelation temperature (Fig. 9). Fig. 9 also shows that, after 13 h, the SA2 gel has not yet reached its final state, and that measuring the modulus at a fixed time after quenching, as previous workers have done, leads to a different relationship between modulus and gelation temperature.

Meunier et al. (1999) have shown that gelation of κ-carrageenan measured at different temperatures can be superimposed to form a unique master curve by suitable shifts along the elasticity and time axes. In the present work, instead of using a reference curve and arbitrary shift factors to build the master curve, we have chosen to use the extrapolated modulus G'_{inf} and $t_{G'=G''}$, as vertical and horizontal shift factors. Using this method, it was noticed that only the horizontal factor, $t_{G'=G''}$, is necessary to produce a reasonable superposition of the curves, as is illustrated in Fig. 10. Clearly, in this figure, only the curve for 40 °C deviates significantly from superposition. It is worth noting that if both parameters (G'_{inf} and $t_{G'=G''}$) are used then an improved scaling is obtained. On the other hand, the use of a G' measured at some specific time after quenching, would lead an apparently larger influence of temperature on final gel properties, and poorer superposition as a result. However, our purpose here is to emphasise that the temperature of gelation overwhelmingly influences the kinetics of gelation, and only has a minor influence on the final gel properties (G'_{inf}). Clearly such a statement can only be valid over a rather limited range of temperature, as above a certain temperature the SA2 is soluble, and gelation will not occur. This master curve can be used to predict gel behaviour for any temperature of gelation in the range studied. It is worthwhile to note that this method can only be used when the gelation kinetics are slower than the time for quenching, otherwise, the gel time cannot be defined.

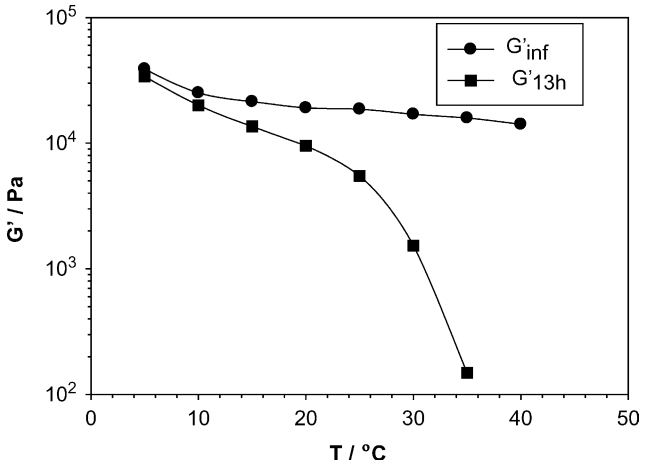

Fig. 9. Gelation-temperature dependence on G' value after 13 h and G'_{inf} of 25% (w/w) SA2 sample (strain amplitude: 0.5%, frequency amplitude: 1 rad/s).

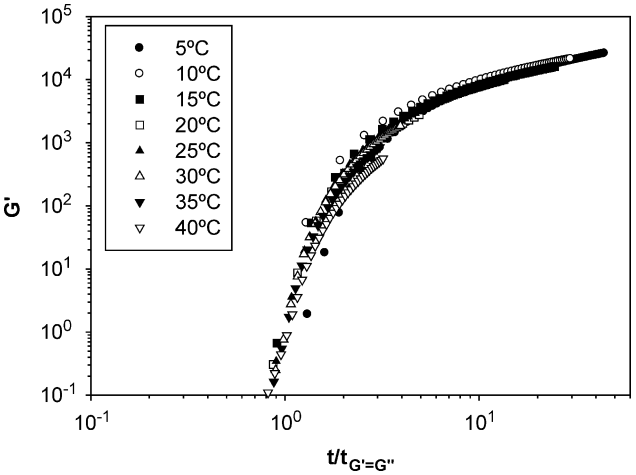

Fig. 10. Master curve with fixed factors ($t_{G'=G''}$) from gelation temperature-dependence of 25% (w/w) SA2 sample (strain amplitude: 0.5%, frequency amplitude: 1 rad/s).

3.5. Influence of concentration on SA2 gelation

Different concentrations of SA2 solutions were prepared and stored in glass vials at 4 °C, and visual observations made of the resulting gels. Below 15%, no sample gelled within a time scale of over 2 months, instead two layers form, i.e. rather than a gel forming, the clear solution turns white, and a sediment forms. It appears that, although the formation of crystallites occurs at concentrations below 15%, they settle out before a network forms, i.e. the volume fraction of crystallites is too small to form a connected, self supporting, network. For 2.5% SA2, the solution becomes turbid but no precipitate is observed.

For concentrations ranging from 17.5 to 40%, the variation of G' and G'' was followed over time. All the solutions were quenched at 10 °C. The oscillatory results for G' are shown in Fig. 11.

From viscosity measurements, the coil overlap concentration, c^*, was found to be around 17%. The closeness of the overlap concentration, c^* and the critical concentration of gelation, c_0 implies that gelation may be considered to occur from an entangled solution on cooling. This idea was

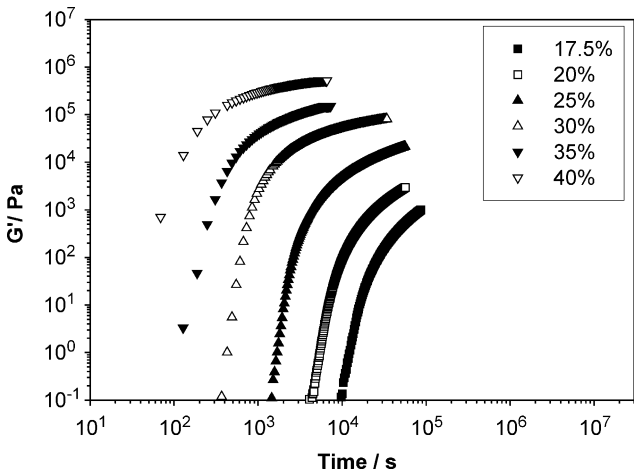

Fig. 11. Influence of concentration (w/w) on gelation behaviour of SA2 sample (strain amplitude: 0.5%, frequency amplitude: 1 rad/s, T_{gel}: 10 °C).

first suggested by Miles, Morris, Ordord, and Ring (1985) for amylose solutions. However, other studies on amylose contradict this suggestion. Doublier and Choplin, 1989 and Gidley (1989) found that the concentration below which no macroscopic amylose gel is formed, c_0, is around 1%, whereas, thanks to viscosity measurements, they determined a value for c^* more than double the critical gelation concentration, c^* i.e. 2–2.5%, depending on the criterion used. Therefore these authors predict that c_0 is not equivalent to c^* and can be much smaller than would be expected from overlap volumes of macromolecular coils.

For concentrations higher than 17.5%, increasing the concentration both increases the gel strength and speeds the kinetics of the gel formation.

As shown in Fig. 12, the time required for formation of a self-supporting network, $t_{G'=G''}$, is found to have a power law dependence on SA2 concentration:

$$\log(t_{G'=G''}) = -6.1\log(c) + 11.7 \quad (2)$$

This power law relation implies a roughly c^{-6} concentration dependence of the gel time for this system, which is similar

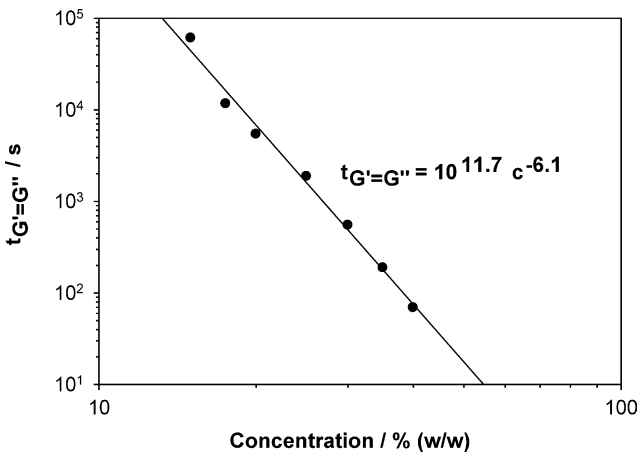

Fig. 12. Concentration-dependence on gel time of SA2 sample (strain amplitude: 0.5%, frequency amplitude: 1 rad/s, T_{gel}: 10 °C).

to the findings of Clark (1995) who found a power law exponent of −5 between log $t_{G'=G''}$ and log c for amylopectin, the branched part of maltodextrin. Clark also observed by X-ray measurements that the course of crystallisation of amylopectin follows a power law dependence on concentration, which is comparable. Kasapis et al. (1993) also found a power law behaviour of 4.5 for SA2, which, whilst it is rather lower than our observed value, is still high compared to the majority of biopolymer gels.

Whilst the first point at 15% may indicate a logarithmic divergence of the gel time, which is expected at the critical gel concentration, an accurate characterisation of this critical region of the gel time–concentration function is difficult, because of the extreme sensitivity of the gels to mechanical disturbance, the extremely long timescales involved and the presence of sedimentation. In particular, sedimentation can lead to high values of G' in the bottom part of the Couette geometry. Therefore, all results below 15% are not shown.

The concentration dependence of the gel modulus is shown in Fig. 13, both for G'_{inf} and $G'_{13\ h}$. One of the earliest attempts to establish a quantitative modulus–concentration relationship for biopolymer gels is due to Hermans (1965). His approach led to the concept of a critical gel concentration, c_0, below which critical branching could not be achieved, and hence gel formation was impossible. Clark and Ross-Murphy (1985) explored the model further, and applied it in a modified cascade theory form. Their method factorises the modulus into two terms, one describing the number of elastically effective chains and the second, the contribution per chain to the modulus. Kasapis et al. (1993) and Manoj et al. (1996, 1997) apply with success the cascade fit to SA2 gelation. Chronakis, Kasapis, and Richardson (1996) also used a modified form of the cascade model and obtain an improved fit to the data. When the cascade model is applied to the present results for SA2 after 13 h gelling, the fit is good but not as good as was achieved with other gels such as gelatin (Clark, 1987)

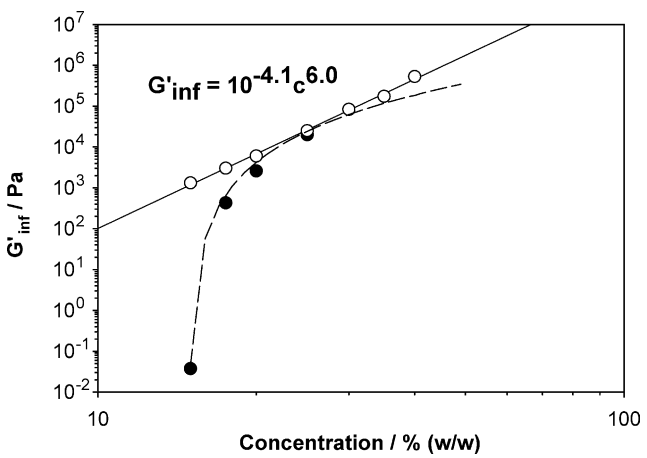

Fig. 13. Concentration-dependence of G' value of SA2 sample (strain amplitude: 0.5%, frequency amplitude: 1 rad/s, T_{gel}: 10 °C). The dotted line shows the cascade fit.

and agarose (Clark, Ross-Murphy, Nishinari, & Watase, 1988). The fit seems to give a good estimation for the critical gel concentration, c_0, which is predicted to be 16%, not far from visual observation, and viscosity measurement data, which predicts the coil overlap concentration, c^* to be 17%. However, the values of G'_{inf} cannot be fitted by the cascade model, hence, any correspondence of the value of c_0, found from the cascade fit, with values from other measurements is probably coincidence. Subsequently, Clark (1995) recognised that the cascade model needs substantial modification to describe microphase-separated biopolymer systems, of which maltodextrin is an example. As can be seen in Fig. 13, the relationship between G'_{inf} and concentration appears to be power law and shows no clear transition towards a critical gel concentration. Nevertheless, as stated before, this could be an artefact due to the extrapolation method of G'_{inf} at low concentrations. Indeed, if the gel formation has not reached its power law regime, the estimated value of G'_{inf} will be larger than the actual value. The difference of behaviour between values of G'_{13h} and G'_{inf} against concentration can also be explained by the kinetics. After 13 h, the low concentration gels have not reached yet the long time power law regime observed at higher concentrations (Fig. 11).

The cascade model also seriously underestimates the sensitivity of gel moduli to changes in concentration in the region of concentration where a power law applies. At high concentrations, when $c/c_0 > 10$, a limiting c^2 relationship between modulus and concentration is predicted by the cascade model. But, since c_0 is predicted to be 16%, this limiting region cannot be accessed experimentally for SA2 and the validity of this prediction cannot be tested. However, in the range of concentrations studied, a linear relation is seen between log G'_{inf} and log c:

$$\log(G'_{inf}) = 6.0 \log(c) - 4.1 \quad (3)$$

This relation shows that the gel properties are strongly concentration dependent, with G' varying as c^6, much higher than the c^2 prediction of the cascade model.

Since the shape of the cure curves at different concentrations is very similar (Fig. 11), an attempt to plot a master curve was made. In previous studies, (Meunier et al. (1999) on κ-carrageenan, Normand et al. (2000a) and Normand, Pudney, Aymard, & Norton (2000b) on gelatin and maltodextrin), concentration master curves have been successfully obtained using free horizontal and vertical shift factors. In the present work, we have chosen to use the extrapolated modulus G'_{inf} and $t_{G'=G''}$, as imposed vertical and horizontal factors. As shown in Fig. 14, this procedure gives an excellent result. When these parameters can be determined, the superposition of the curves demonstrates that the shape of the time course of gelation for SA2 is universal and characterised by two fundamental parameters: G'_{inf} and $t_{G'=G''}$.

Within the experimental error, both G'_{inf} and $t_{G'=G''}$ have a power law dependence on the concentration: $G'_{inf} \propto C^{6.0}$ and $t_{G'=G''} \propto C^{-6.1}$. As far as the concentration dependence of the shear modulus (vertical shift factors) is concerned, our result is in good agreement with that found by Normand et al. (2000b) ($G'_{inf} \propto C^{5.6}$). However, the same cannot be said for the concentration dependence of the horizontal shift factors, here, a bigger discrepancy was found compared to Normand et al. (2000b), who found $t_{G'=G''} \propto C^{-1.9}$. This difference could be attributed to the fact that in our experiments, we have used a temperature quench instead of temperature ramps. Quenching allows us to study the kinetics of gelation accurately, and to reduce the time necessary to reach the final equilibrium temperature (here 10 °C). Indeed, as we have shown above (Figs. 7 and 8), the kinetics are strongly temperature-dependent. Thus, using temperature ramps will increase uncertainty of the cure curve shapes in the earlier stage of the gelation and may lead to erroneous superimposition shift factors.

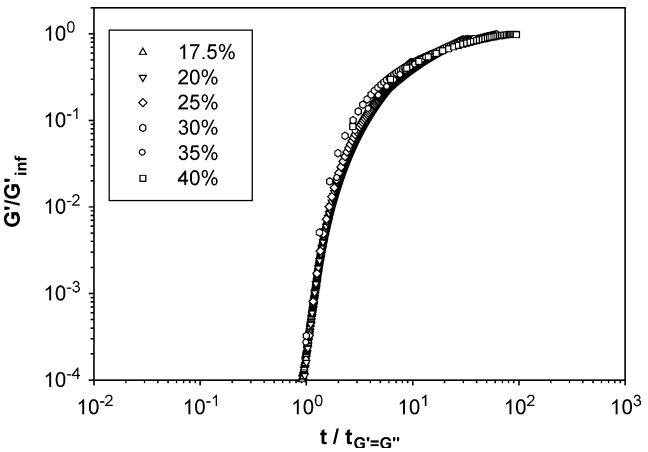

Fig. 14. Master curve with fixed shift factors (G'_{inf} and $t_{G'=G''}$) on concentration-dependence of SA2 gel (strain amplitude: 0.5%, frequency amplitude: 1 rad/s, T_{gel}: 10 °C).

From a more general point of view, the fact that a master curve can be drawn from individual cure curves implies that the concentration does not change the structure of the gel. Furthermore, increasing the concentration increases the number and the density of junction points and accelerates kinetics of gel formation. Hence, it appears that, at different concentrations, the same structure is formed but faster when concentration increases, and with different aggregate density.

Such apparently self-similar behaviour is consistent with the fractal nature of networks formed by aggregation processes in colloidal suspensions. In such systems, experiment and theory have shown that both the gel time (Trompette & Meireles, 2003) and modulus (Buscall et al., 1987; Krall & Weitz, 1998) will display a power law dependence on concentration, as has been observed here. It should be noted, however, that the experimental observation and theoretical predictions display power laws of at most 4 for both the gel time and modulus, and are thus rather lower than those observed here. Despite this caveat, it does

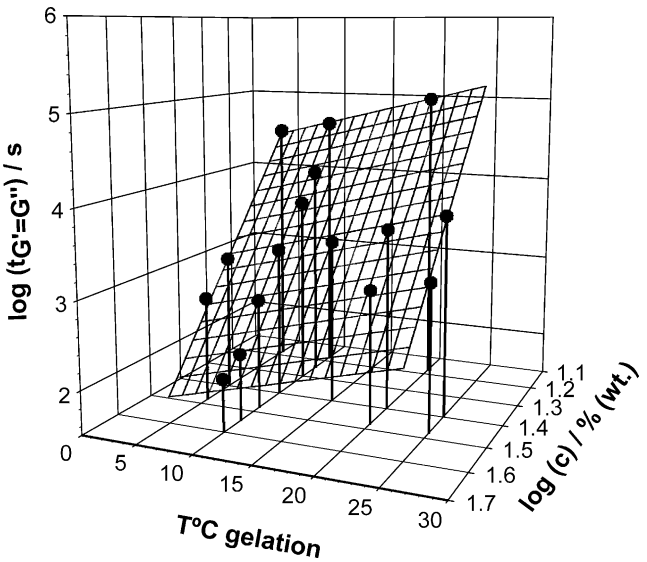

Fig. 15. Effect of gelation temperature and concentration on gel time of SA2 sample (strain amplitude: 0.5%, frequency amplitude: 1 rad/s).

appear that SA2 gels can be better described as a particulate gel rather than a polymer network gel.

3.6. Influence of gelation temperature and concentration on SA2 gelation

From the previous data on the effect of temperature and concentration on the mechanical properties of SA2 gels, and in particular on the gel time ($t_{G'=G''}$), a linear equation relating the three parameters is obtained:

$$\log(t_{G'=G''}) = 0.031\mathrm{T} - 6.1\log(c) + 11.5 \quad (4)$$

This is a similar procedure to one previously used by Kasapis et al. (1993) although our data are more extensive and determined rheometrically rather than by visual observation. The prediction from Eq. (4) is compared with the data in Fig. 15. Clearly, this can then be used to predict the maltodextrin gelation time for different concentrations at different temperatures of processing, over the experimentally accessible range of concentrations (15–40%) and temperatures (5–25 °C) studied.

4. Conclusion

A detailed rheological analysis of maltodextrin gels has been conducted, extending previous work on the system and demonstrating some previously unobserved phenomena. We find that the dissolution temperature has a major influence on gelation behaviour, which may be due to the temperature dependence of the concentration of active nuclei. The temperature of gelation also has a significant influence on the kinetics (i.e. on $t_{G'=G''}$) but much less so on the final modulus of gelation (G'_{inf}) so long as the temperature is well below the critical gelation temperature. We also note that the concentration dependence of both $t_{G'=G''}$ and G'_{inf} display power law behaviour of approximately $1/c^6$ and c^6, respectively. Previous studies have taken modulus data as a function of concentration at a specific time after the start of the experiment, and have seen different concentration dependence as a result. Because of this difference we find that the cascade model does not fit our data. Despite the mechanism of gelation of maltodextrin appearing to be quite complex, it was possible to obtain a master curve for concentration and temperature dependence. As a result, these master curves, together with a single elasticity measurement at one temperature and one concentration, can be used to predict the entire gelation behaviour, at any concentration or temperature within the range studied here.

Acknowledgements

The authors gratefully acknowledge many useful discussions with Allan H. Clark.

References

Bulpin, P. V., Cutler, A. N., & Dea, I. C. M. (1984). Thermally-reversible gels from low DE maltodextrins. In G. O. Phillips, P. A. Williams, & D. J. Wedlock (Eds.), *Gums and stabilisers for the food industry 2* (pp. 475–484). Oxford: IRL Press.

Buscall, R., McGowan, I. J., Mills, P. D. A., Stewart, R. F., Sutton, D., White, L. R., & Yates, G. E. (1987). The rheology of strongly-flocculated suspensions. *Journal of Non-Newtonian Fluid Mechanics*, *24*(2), 183–202.

Chronakis, I. S., Kasapis, S., & Richardson, R. K. (1996). Small deformation rheological properties of maltodextrin–milk protein systems. *Carbohydrate Polymers*, *29*(2), 137–148.

Clark, A. H. (1987). The application of network theory to food systems. In: *Food structure and behaviour*, p. 13–34.

Clark, A. H. (1995). Application of cascade theory to the description of microphase-separated biopolymer gels. *Faraday Discussions*, *101*, 77–91.

Clark, A. H., Gidley, M. J., Richardson, R. K., & Ross-Murphy, S. B. (1989). Rheological studies of aqueous amylose gels—the effect of chain-length and concentration on gel modulus. *Macromolecules*, *22*(1), 346–351.

Clark, A. H., & Ross-Murphy, S. B. (1985). The concentration-dependence of bio-polymer gel modulus. *British Polymer Journal*, *17*(2), 164–168.

Clark, A. H., Ross-Murphy, S. B., Nishinari, K., & Watase, M. (1988). Shear modulus–concentration relationships for biopolymers gels. Comparison of independent and cooperative crosslink descriptions. In: *Physical networks: polymers and gels*, Elsevier Applied Science, pp. 209–229.

Croguennoc, P., Meunier, V., Durand, D., & Nicolai, T. (2000). Characterization of semidilute kappa-carrageenan solutions. *Macromolecules*, *33*(20), 7471–7474.

Doublier, J. L., & Choplin, L. (1989). A rheological description of amylose gelation. *Carbohydrate Research*, *193*, 215–226.

Ferry, J. D. (1980). *Viscoelastic properties of polymers* (3rd ed.). New York: Wiley.

German, M. L., Blumenfeld, A. L., Guenin, Y. V., Yuriev, V. P., & Tolsguvoz, V. B. (1992). Structure formation in systems containing

amylose, amylopectin, and their mixtures. *Carbohydrate Polymers*, *18*(1), 27–34.

Gernat, C., Reuther, F., Damaschun, G., & Schierbaum, F. R. (1987). Real structure of a partially crystalline maltodextrin gel as revealed by wide-angle x-ray-scattering. *Acta Polymerica*, *38*(11), 603–607.

Gidley, M. J. (1989). Molecular mechanisms underlying amylose aggregation and gelation. *Macromolecules*, *22*(1), 351–358.

GluckHirsch, J. B., & Kokini, J. L. (1997). Determination of the molecular weight between crosslinks of waxy maize starches using the theory of rubber elasticity. *Journal of Rheology*, *41*(1), 129–139.

Hermans, J. (1965). Investigation of the elastic properties of the particle network in gelled solutions of hydrocolloids I carboxymethyl cellulose. *Journal of Polymer Science*, *3*, 1859–1868.

Kasapis, S., Morris, E. R., Norton, I. T., & Clark, A. H. (1993). Phase-equilibria and gelation in gelatin maltodextrin systems.1. Gelation of individual components. *Carbohydrate Polymers*, *21*(4), 243–248.

Krall, A. H., & Weitz, D. A. (1998). Internal dynamics and elasticity of fractal colloidal gels. *Physical Review Letters*, *80*(4), 778–781.

Launay, B., Doublier, J. L., & Cuvelier, G. (1986). Flow properties of aqueous solutions and dispersions of polysaccharides. In: *Functional properties of foods macromolecules*, Amsterdam: Elsevier Applied Science, pp. 1–78.

Manoj, P., Kasapis, S., & Chronakis, I. S. (1996). Gelation and phase separation in maltodextrin–caseinate systems. *Food Hydrocolloids*, *10*(4), 407–420.

Manoj, P., Kasapis, S., & Hember, M. W. N. (1997). Sequence-dependent kinetic trapping of biphasic structures in maltodextrin–whey protein gels. *Carbohydrate Polymers*, *32*(2), 141–153.

Meunier, V., Nicolai, T., Durand, D., & Parker, A. (1999). Light scattering and viscoelasticity of aggregating and gelling kappa-carrageenan. *Macromolecules*, *32*(8), 2610–2616.

Miles, M. J., Morris, V. J., Ordord, P. D., & Ring, S. G. (1985). The roles of amylose and amylopectin in the gelation and retrogradation of starch. *Carbohydrate Research*, *135*(2), 271–281.

Moates, G. K., Noel, T. R., Parker, R., & Ring, S. G. (1997). The effect of chain length and solvent interactions on the dissolution of the b-type crystalline polymorph of amylose in water. *Carbohydrate Research*, *298*(4), 327–333.

Morris, E. R. (1984). Rheology of hydrocolloids. In G. O. Phillips, P. A. Williams, & D. J. Wedlock (Eds.), *Gums and stabilisers for the food industry 2* (pp. 57–78). Oxford: IRL Press.

Morris, E. R., Cutler, A. N., Ross-Murphy, S. B., & Rees, A. (1981). Concentration and shear rate dependence of viscosity in random coil polysaccharide solutions. *Carbohydrate Polymers*, (1), 5–21.

Normand, V., Muller, S., Ravey, J. C., & Parker, A. (2000a). Gelation kinetics of gelatin: a master curve and network modeling. *Macromolecules*, *33*(3), 1063–1071.

Normand, V., Pudney, P. D. A., Aymard, P., & Norton, I. T. (2000b). Weighted-average isostrain and isostress model to describe the kinetic evolution of the mechanical properties of a composite gel: application to the system gelatin: maltodextrin. *Journal of Applied Polymer Science*, *77*(7), 1465–1477.

Reuther, F., Damaschun, G., Gernat, C., Schierbaum, F. R., Kettlitz, B., Radosta, S., & Nothnagel, A. (1984). Molecular gelation mechanism of maltodextrins investigated by wide-angle x-ray-scattering. *Colloid and Polymer Science*, *262*(8), 643–647.

Reuther, F., Plietz, P., Damaschun, G., Purschel, H. V., Krober, R., & Schierbaum, F. R. (1983). Structure of maltodextrin gels-a small-angle x-ray-scattering study. *Colloid and Polymer Science*, *261*(3), 271–276.

Richardson, R. K., Robinson, G., Ross-Murphy, S. B., & Todd, S. (1981). Mechanical spectroscopy of filled gelatin gels. *Polymer Bulletin*, *4*(9), 541–546.

Ritcher, M., Schierbaum, F. R., Augustat, S., & Knoch, K. D (1976). Method of producing starch hydrolysis products use as food additives (patent number: 3962465).

Robin, J. P., Mercier, C., Charbonniere, R., & Guilbot, A. (1974). Lintnerized starches gel-filtration and enzymatic studies of insoluble residues from prolonged acid treatment of potato starch. *Cereal Chemistry*, *51*(3), 389–406.

Schierbaum, F. R., Radosta, S., Vorwerg, W., Yuriev, V. P., Braudo, E. E., & German, M. L. (1992). Formation of thermally reversible maltodextrin gels as revealed by low resolution h-nmr. *Carbohydrate Polymers*, *18*(3), 155–163.

Trompette, J. L., & Meireles, M. (2003). Ion-specific effect on the gelation kinetics of concentrated colloidal silica suspensions. *Journal of Colloid and Interface Science*, *263*(2), 522–527.

Vorwerg, W., & Radosta, S. (1995). Rheological investigation of starch polysaccharide gelation. *Macromolecular Symposia*, *99*, 71–82.

Winter, H. H., & Chambon, F. (1986). Analysis of linear viscoelasticity of a cross-linking polymer at the gel point. *Journal of Rheology*, *30*(2), 367–382.